JPNT *Journal of Positioning, Navigation, and Timing*

Threshold Determination of The GPS Carrier Acceleration, Ramp, and Step on the Normal Condition

Eunseong Son[†], Koon−Tack Kim, Sung−Hyuck Im, Moon Beom Heo
Department of Satellite Navigation Team, Korea Aerospace Research Institute, Daejeon 34133, Korea

ABSTRACT

In this study, the carrier acceleration-ramp-step test was applied to GPS carrier phase measurements, and the results were compared and analyzed. In the carrier acceleration-ramp-step test, the acceleration, ramp, and measurements are estimated using 10 consecutive carrier phase measurements for satellites observed at the same time based on the least square method. As for the characteristic of this test, if failure occurs in the measurement, the value jumps significantly compared to the previous result; but it judges that failure has occurred in all the satellites although failure has occurred in one satellite. Therefore, in this study, a method that eliminates a satellite with failure was suggested, and thresholds of the carrier acceleration, ramp, and step were suggested. The evaluation of the failure detection performance of carrier phase measurement using the suggested thresholds showed that failure could be detected when the carrier phase measurement changed abruptly by more than about 0.1 cycles.

Keywords: GNSS, carrier phase, acceleration, ramp, step, threshold

1. INTRODUCTION

A Global Navigation Satellite System (GNSS) was developed for military purposes, but it is currently also used in various civilian fields (e.g., land transportation, shipping, and aviation) (Son et al. 2013). GNSS can determine the position of a receiver using the measurements of signals received from at least four satellites. Accordingly, GNSS is used for positioning in relation to traffic, geodetic survey, and surveying, and also widely used for time synchronization, weather monitoring, etc. (Lee et al. 2013). The economic and social importance of GNSS is well known. Therefore, many countries in the world have made efforts to establish their own GNSS. Starting with the Global Positioning System (GPS) from the United States, the development of the GLObal NAvigation Satellite System from Russia has been completed; and Galileo from Europe,

Beidou from China, the Quasi-Zenith Satellite System from Japan, and the Indian Regional Navigation Satellite System from India are under development.

The performance requirements for positioning using GNSS are divided into accuracy, integrity, continuity, and availability (Lee et al. 2013). To secure the reliability of these requirements, it is necessary to detect the failure of a satellite and to eliminate the detected measurement. Quality Monitoring (QM) is a well-known method for detecting the failure of a satellite, and it can be divided into Signal QM, Data QM, and Measurement QM (Gang 2004, Koenig 2010).

For positioning using GPS, pseudorange and carrier phase measurements are used. However, they include ionosphere, troposphere, and multipath errors, and precise positioning cannot be performed if these errors are not eliminated. Therefore, many studies have been actively performed to eliminate GPS error sources. In this study, the carrier acceleration-ramp-step test was conducted, which is a pre-processing phase before performing an algorithm for eliminating the errors or precise positioning.

As previous research on the carrier acceleration-ramp-

step test, Gang (2004) performed the carrier acceleration-ramp-step test with the purpose of developing an Integrity Monitor Testbed (IMT) which is a prototype of the Local Area Augmentation System. However, Gang (2004) did not numerically suggest thresholds of acceleration, ramp, and step, respectively, based on the results of the test. Also, Gang (2004) suggested a countermeasure for the occurrence of failure in the carrier phase measurement, but results for actual failure or artificially induced failure were not presented. To compare the Joint Precision and Approach Landing System (JAPLS) Testbed Platform, which is a prototype of the JPALS, and existing IMT, Koenig (2010) suggested a new algorithm that improved the existing carrier acceleration-ramp-step algorithm. However, Koenig (2010) mentioned that the carrier acceleration-ramp-step test is also useful for the detection of a cycle slip, but results for the occurrence of cycle slip were not presented.

In this study, determination of thresholds for the failure detection of carrier phase measurement using the carrier acceleration-ramp-step algorithm suggested by Koenig (2010) was investigated. In the case of the thresholds, root mean square (RMS) was calculated for each test result, and analysis was performed by dividing the satellite elevation angle. Also, problems occurring in the data processing procedure, results obtained in case of failure, and whether the algorithm can detect a cycle slip were described.

2. DATA PROCESSING AND ANALYSIS

2.1 Carrier Acceleration-Ramp-Step Test

The carrier acceleration-ramp-step test examines rapid changes in the carrier phase measurements. To examine the cause for the case where the thresholds of the acceleration, ramp, and step for carrier phase measurements are exceeded, this test establishes 10 consecutive measurement test windows. This is because there is an ambiguity about whether it is failure for the measurement or failure due to the change in visible satellites, if a test window is not established (Gang 2004).

When the signal transmitted from the satellite s has reached to the receiver, r, the carrier phase measurement equation can be expressed as Eq. (1). In Eq. (1), ρ is the geometry range, c is the speed of light, t^s is the receiver clock error, I is the satellite clock error, T is the ionospheric error, λ is the tropospheric error, N is the wavelength, is the integer ambiguity, and is the measurement noise in unit of meters. Besides the errors expressed in Eq. (1), there are phase center variation of the satellite and receiver antenna, site displacements, and multipath errors, but they were not considered in this study (Son 2013).

$$\Phi_r^s = \rho_r^s + c\left(t_r - t^s\right) - I_r^s + T_r^s + \lambda N_r^s + \varepsilon_r^s \tag{1}$$

The carrier acceleration-ramp-step test uses 10 consecutive measurements, and the same number of satellites should be applied. The targets of the test are the terms on the right side of Eq. (2). In Eq. (2), carrier phase measurement is known to have very low noise, and thus it was excluded from the measurement equation.

$$\Phi_{r,c}^s = \Phi_r^s - \rho_r^s + ct^s = ct_r - I_r^s + T_r^s + \lambda N_r^s \tag{2}$$

To eliminate the receiver clock error in Eq. (2), the measurements of the satellites observed at the same time were averaged, and differencing with Eq. (2) was then performed as shown in Eq. (3). For this averaging, 10 consecutive measurements need to be averaged based on the same number of satellites. If the number of satellites is different for even one value among the 10 consecutive measurements, the carrier acceleration-ramp-step test judges that there is a failure.

$$\Phi_{r,\text{diff}}^s = \Phi_{r,c}^s - \Phi_{r,\text{avg}}^s \tag{3}$$

The acceleration-ramp-step test is shown in Eq. (4), where a_2 is the acceleration, a_1 is the ramp, and a_0 is the estimated measurement. Thus, the step test is the difference between the actual carrier phase measurement and the estimated value, as shown in Eq. (5).

$$\hat{\Phi}_{r,\text{diff}}^s = a_0 + a_1 n + \frac{1}{2} a_2 n^2 \tag{4}$$

$$Step = \hat{\Phi}_{r,\text{diff}}^s - \Phi_{r,\text{diff}}^s = a_0 + a_1 n + \frac{1}{2} a_2 n^2 - \Phi_{r,\text{diff}}^s \tag{5}$$

The acceleration, ramp, and estimated measurement can be estimated using the least-square method as shown in Eq. (6), and the design matrix is expressed in Eq. (7) (Koenig 2010).

$$\hat{\Phi}_{r,\text{diff}}^s = \left(H^T H\right)^{-1} H^T \Phi_{r,\text{diff}}^s \tag{6}$$

$$H = \begin{bmatrix} 1 & 1 & \frac{1}{2}1^2 \\ 1 & 2 & \frac{1}{2}2^2 \\ \vdots & \vdots & \vdots \\ 1 & 10 & \frac{1}{2}10^2 \end{bmatrix} \tag{7}$$
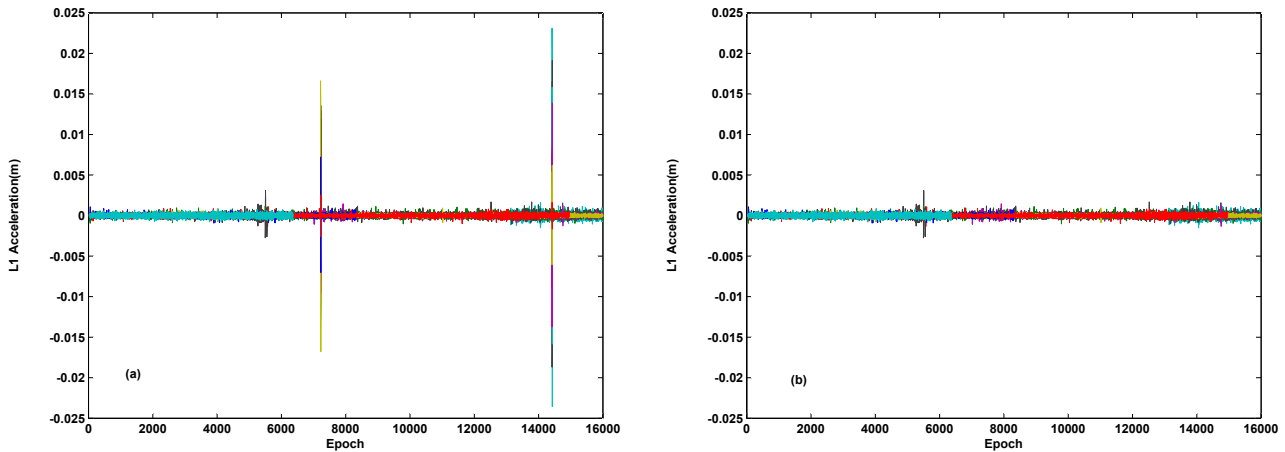
Fig. 1. Result of non-adjusted geometry range and satellite clock error (a) and of adjusted geometry range and satellite clock error (b).

2.2 Analysis of The Test Result

The carrier acceleration-ramp-step test was carried out using the equations listed in Section 2.1. The GPS data used for the test were obtained from the GNSS permanent stations built by the Korea Aerospace Research Institute, which are located in Anseong, Boeun, Daejeon, Eumseong, and Gongju. At each permanent station, identical GNSS dual-frequency receiver and choke ring antenna with radome are installed. These data are stored at one second intervals based on the Coordinated Universal Time, and the minimum satellite elevation angle is set to 5 degrees.

As shown in Eq. (2), the carrier acceleration-ramp-step test judges the failure of ionospheric/tropospheric errors and integer ambiguity. The ionosphere is the largest error source for GPS after removing the Selective Availability. This is affected by the electromagnetic energy emitted from the Sun, and thus, in Korea, the effect is large in the summer. The troposphere exists at the lower part of the atmosphere, and the tropospheric delay can be divided into dry delay and wet delay. Among them, wet delay is affected by water vapor, and thus, in this study, data in the summer season in Korea with high temperature and humidity that are thought to have large ionospheric and tropospheric errors were used. Seven-day data between July 2 and 8, 2015 (DOY, Day of Year 182~188) were used; and in the case of the analysis method, RMS values were compared and analyzed for each permanent station and satellite.

For the carrier acceleration-ramp-step test, the geometry range between the GPS satellite and the receiver needs to be known as shown in Eq. (2). To obtain the geometry range, the coordinates of the satellite and the precise coordinates of the receiver need to be known. Therefore, in this study, the coordinates of the satellite was calculated using GPS

Subframes 1, 2, and 3 assuming a real-time system, and the precise coordinates of the permanent station was obtained based on Bernese 5.0 which is precise GNSS data processing software.

The result of the carrier acceleration-ramp-step test indicated that the value jumped at about 7200 second intervals as shown in Fig. 1a. The examination of the result indicated that there was difference in the geometry range and satellite clock errors as the broadcast ephemeris was updated about every two hours. Therefore, to eliminate this false detection, the geometry range and satellite clock errors calculated using the past broadcast ephemeris were adjusted based on the newly updated broadcast ephemeris. As a result, the values that jump at about two hour intervals disappeared as shown in Fig. 1b.

Using the algorithm that adjusted the geometry range and satellite clock errors, the L1 carrier acceleration-ramp-step test results for PRN1 and PRN24 on DOY 183 at the Boeun permanent station were presented in Figs. 2 and 3, respectively. In Fig. 2, the acceleration, ramp, and step values gradually decreased depending on the satellite elevation angle; but in Fig. 3, the remaining values excluding the ramp with a satellite elevation angle of less than about 15 degrees showed similar distributions regardless of the satellite elevation angle.

To examine if the acceleration, ramp, and step values are related with the satellite elevation angle, RMS was calculated for each value by dividing the satellite elevation angle into 15 degree intervals. Table 1 summarizes the maximum value of averaged RMS for each satellite calculated for the analysis period depending on each permanent station and satellite elevation angle. As for the L1 results in Table 1, most acceleration values were uniform excluding the satellite elevation angle of 5 to 15 degrees,
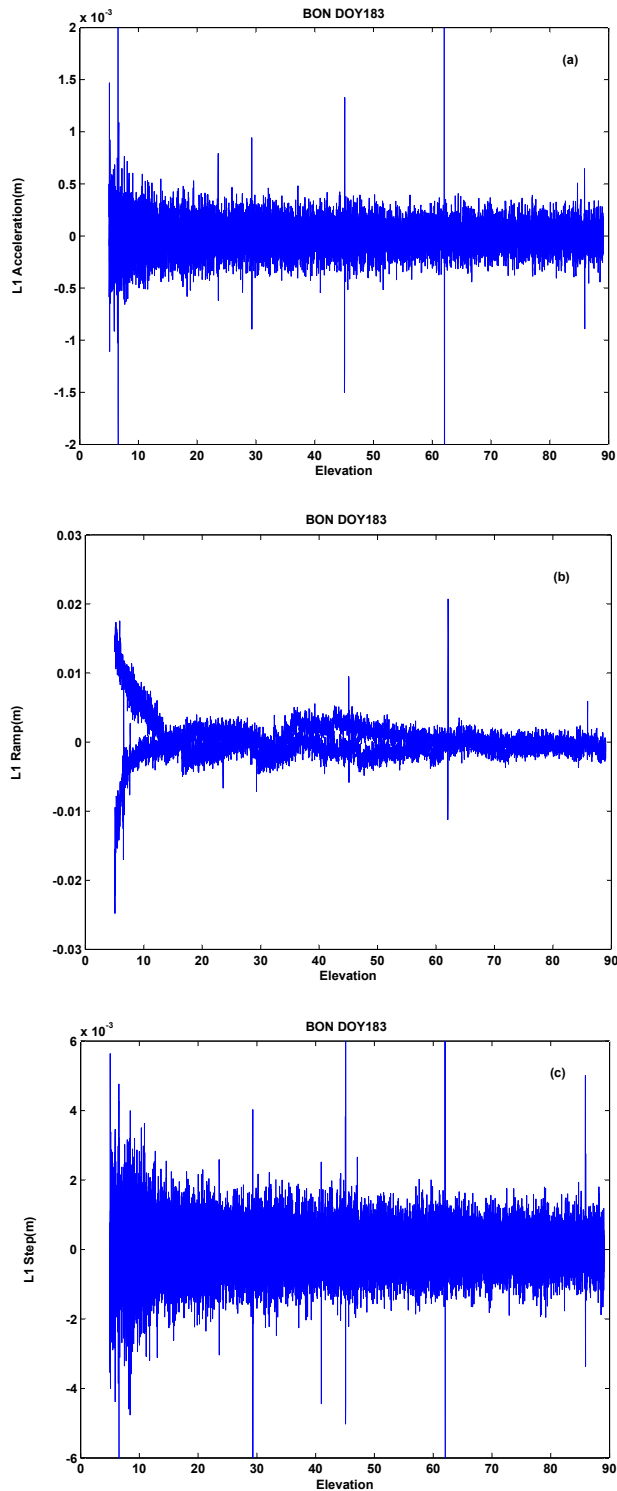
Fig. 2. PRN1's L1 acceleration (a), ramp (b), and step (c) at BON.

Fig. 3. PRN24's L1 acceleration (a), ramp (b), and step (c) at BON.

and the ramp and step values were the largest at the satellite elevation angle of 5 to 15 degrees in every permanent station. Also, the RMS value generally decreased as the satellite elevation angle increased although the trend was gentle. However, in the case of L2, it was not easy to find a

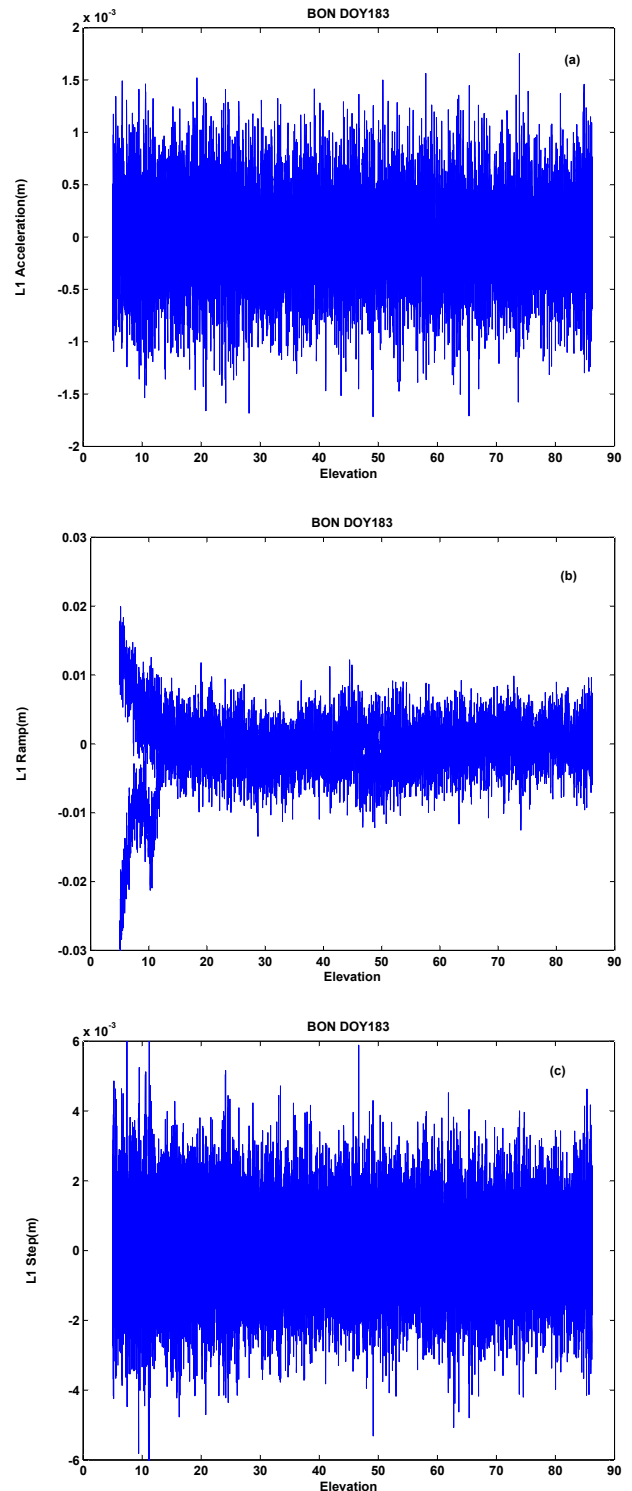constant pattern excluding the Daejeon permanent station. In particular, the Anseong permanent station showed a very large difference between L1 and L2.

The examination of the Anseong permanent station in relation to the L2 result in Table 1 showed that a failure of

Table 1. The maximum value of averaged RMS in 7 days of satellite for L1, L2.

| Elev.(°) Sta.	Acceleration (10^{-1} m)						Ramp (10^{-3} m)						Step (10^{-3} m)					
	5~15	15~30	30~45	45~60	60~75	75~90	5~15	15~30	30~45	45~60	60~75	75~90	5~15	15~30	30~45	45~60	60~75	75~90
ANS L1	10	5	5	5	4	5	11	4	4	4	3	3	8	2	1	2	1	1
BON L1	5	5	5	5	4	4	11	4	5	4	3	3	2	1	1	1	1	1
DAE L1	5	5	5	5	4	4	12	5	5	4	3	3	2	1	1	1	1	1
EUM L1	18	5	10	7	4	5	12	4	7	5	4	3	15	2	4	3	2	2
GNJ L1	21	5	5	5	4	4	15	4	5	4	3	3	17	2	3	3	2	1
ANS L2	368	24	38	39	15	44	219	15	23	23	10	26	153	10	16	16	7	18
BON L2	50	7	12	10	8	5	35	6	9	8	7	3	16	2	4	3	3	1
DAE L2	6	5	5	5	4	5	12	4	4	4	3	3	3	2	1	1	1	1
EUM L2	83	12	14	13	10	10	47	8	9	8	6	6	37	5	5	5	4	5
GNJ L2	128	15	14	16	15	5	75	9	7	10	10	3	88	8	9	9	8	1
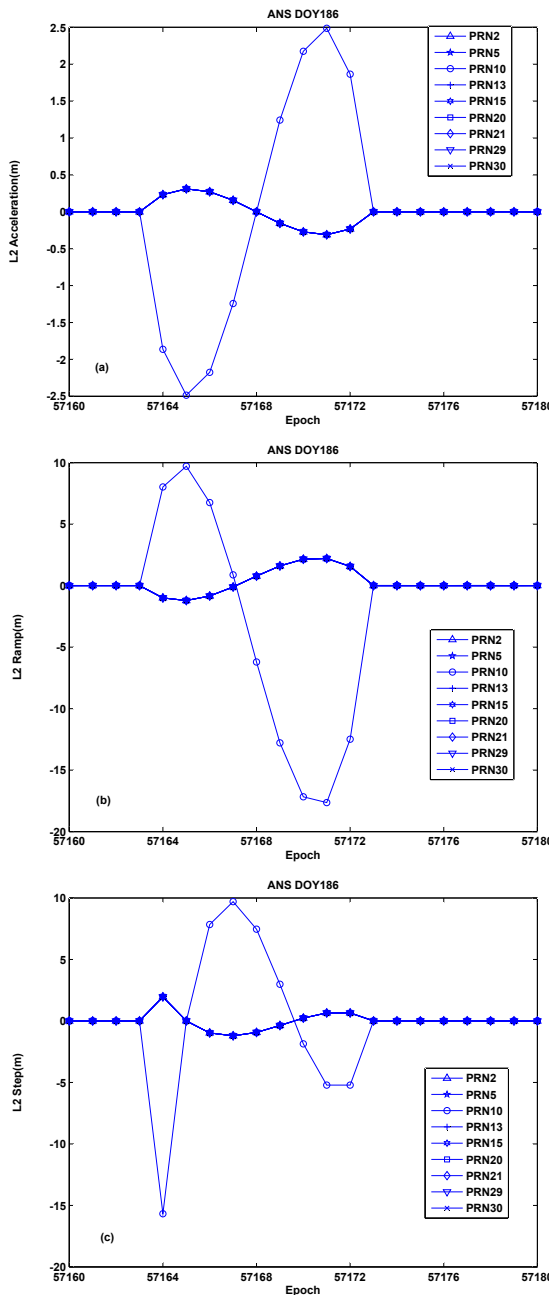
Fig. 4. The L2 measurement fault of the acceleration (a), ramp (b), and step (c) at ANS.

about 2.5 m was observed at the acceleration part, and a failure of about 20 m was observed at the ramp and step parts of PRN10 on DOY 186. Considering that the satellite elevation angle of PRN10 was about 8 degrees, it is thought that an abrupt change such as ionospheric/tropospheric errors or a cycle slip occurred. However, as shown in Fig. 4, the values of all the satellites jumped at epoch 57163, and it occurred in the acceleration, ramp, and step values in common. This is because all the satellites were affected by the averaging for eliminating the receiver clock error in Eq. (3) (Gang 2004). Also, as 10 consecutive measurement test windows were established, failure occurred consecutively in 10 epochs.

2.3 Detection of Cycle Slip

Koenig (2010) mentioned that the carrier acceleration-ramp-step test is also useful for the detection of a cycle slip. However, Koenig (2010) did not present analysis results for a cycle slip. Therefore, in this study, the changes in the acceleration, ramp, and step depending on the cycle slip were analyzed by adding an artificial cycle slip to the carrier phase measurement. In the case of the data used for cycle slip detection, DOY183 data from the Daejeon permanent station were used. The cycle slip of carrier phase measurement occurs in integer multiples (Hofmann-Wellenhof et al. 2008). Thus, in the case of the L1 measurement, one cycle (i.e., the minimum unit of a cycle slip) was artificially added to PRN4, and the result was shown in Fig. 5. The result of the one cycle slip addition showed that the values jumped to about 0.01 m for the acceleration, about 0.07 m for the ramp, and about 0.07 m for the step; and it was consecutively observed at 10 measurements similar to the result shown in Fig. 4. Also, it affected the other satellites, but the jump was the largest for PRN4 to which the cycle slip had been added. The artificial addition of 100 cycles to the L2 measurement showed that the value jumped to about 1.4 m, indicating that the amount of jump increased as the number of cycle slips increased.
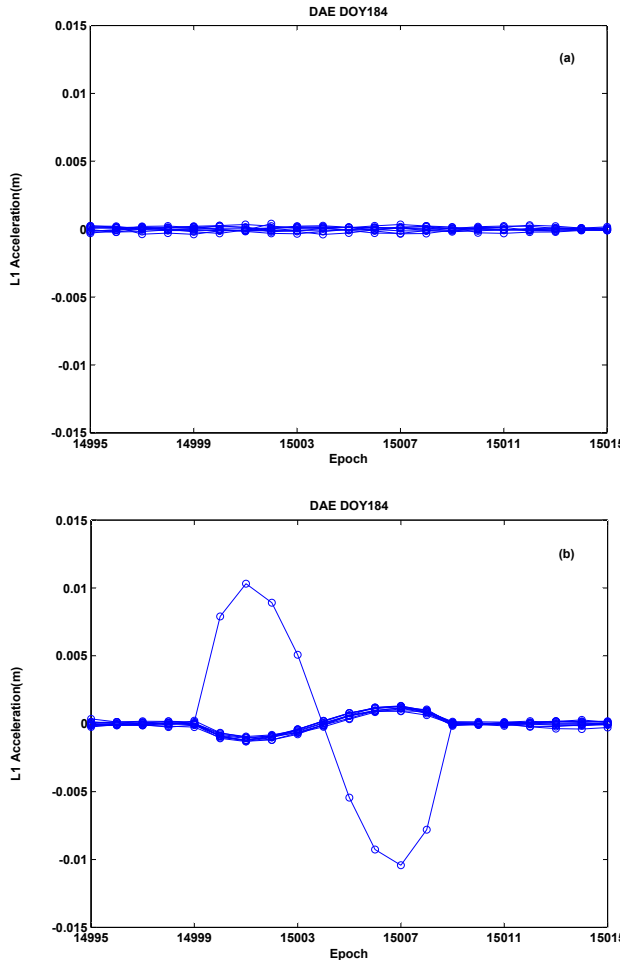
Fig. 5. Case of non-cycle slip (a) and cycle slip (b) of L1's acceleration at DAE.

3. THRESHOLD DETERMINATION

3.1 Strategy for Prevent a Fault in All Satellite

The result of the analysis in Section 2 showed that when failure occurs in the carrier phase measurement, the carrier acceleration-ramp-step test affects all the satellites. Thus, if failure detection is conducted without considering this effect, it is judged that failure has occurred in all the satellites, and this would decline the availability of the satellites without an actual failure. Also, for a system that is operated in real time, all the satellites cannot be used or the quality of the result would deteriorate. Accordingly, it is necessary to prevent it from judging that failure has occurred in all the satellites. The examination showed that when failure occurred in a specific satellite, the value jumped to the opposite direction compared to the other satellites without a failure. Therefore, for the test results of the analysis period, the visible satellites were compared at the same epoch, and one satellite with a different sign was extracted and eliminated. Then, recalculation was performed, and the results were summarized in Table 2. As summarized in Table 2, the acceleration showed very similar values for each permanent station and satellite elevation angle, and the values of L2 were larger than those of L1. However, after the satellite elevation angle of 60 degrees, there was no large difference between L1 and L2. In the case of the ramp, it was about 0.011 m at the satellite elevation angle of 5 to 15 degrees, which was much larger than the values at the remaining satellite elevation angles. The values showed a slight difference depending on the satellite elevation angle, where it was about 0.004 m at 15 to 60 degrees and about 0.003 m at 60 to 90 degrees. However, there was no large difference in the ramp between L1 and L2. In the case of the step, the value at the satellite elevation angle of 5 to 15 degrees was larger than those at the remaining satellite elevation angles, and the difference between L1 and L2 was the largest.

3.2 Threshold Setting and Evaluation

To examine if the carrier acceleration-ramp-step test values are related with the satellite elevation angle, the figures for the PRN1 and PRN24 of the Boeun permanent

**Table 2.** The maximum value of averaged RMS in 7 days of satellite for L1, L2.

Elev.(°) Sta.	Acceleration (10^{-4} m)						Ramp (10^{-3} m)						Step (10^{-4} m)					
	5~15	15~30	30~45	45~60	60~75	75~90	5~15	15~30	30~45	45~60	60~75	75~90	5~15	15~30	30~45	45~60	60~75	75~90
ANS L1	5	4	4	4	4	4	11	4	4	4	3	3	16	14	13	13	12	13
BON L1	5	4	4	4	4	4	11	4	4	4	3	3	17	14	14	13	13	13
DAE L1	5	5	4	4	4	4	12	5	5	4	3	3	15	14	13	13	13	13
EUM L1	5	4	4	4	4	4	10	4	4	4	3	3	15	14	13	13	13	12
GNJ L1	5	4	4	5	4	4	11	4	5	4	3	3	15	14	13	14	13	12
ANS L2	6	5	5	5	4	4	11	4	4	4	3	3	27	15	14	14	13	13
BON L2	6	5	5	5	4	4	12	4	4	4	3	3	22	15	14	14	13	13
DAE L2	5	5	5	5	4	4	12	4	4	4	3	3	23	15	14	14	13	13
EUM L2	5	5	4	5	4	4	10	4	4	4	3	3	21	15	13	14	13	13
GNJ L2	5	5	5	5	4	4	12	4	4	4	4	3	20	15	14	14	13	13

Table 3. Threshold of the acceleration, ramp, and step.

Elevation Angle (°)	L1 (m)			L2 (m)		
	Acceleration	Ramp	Step	Acceleration	Ramp	Step
5~15	±0.0010	±0.025	±0.0035	±0.0012	±0.025	±0.0055
15~30	±0.0009	±0.010	±0.0030	±0.0010	±0.010	±0.0033
30~45	±0.0009	±0.010	±0.0028	±0.0010	±0.010	±0.0030
45~60	±0.0009	±0.009	±0.0028	±0.0010	±0.009	±0.0030
60~75	±0.0008	±0.008	±0.0026	±0.0008	±0.008	±0.0028
75~90	±0.0008	±0.008	±0.0026	±0.0008	±0.008	±0.0028

station were presented in Section 2.3. As shown in the figures, the test result values of PRN24 were larger than those of PRN1. The examination of the results from all the permanent stations during the analysis period showed that all the values of PRN24 were larger than those of the other satellites, and thus the RMS values were also larger than those of the other satellites. To examine the abnormality of PRN24, Notice Advisory to NAVSTAR Users, the satellite health of the broadcast ephemeris, and the International GNSS Service precise ephemeris for the analysis period were searched, but there was no particular remark. Therefore, in this study, the results of positioning using L1 single-RTK were compared between the case including PRN24 and the case without PRN24. The data used for the positioning was an atomic clock station that is about 40 m apart from the Daejeon permanent station. At the atomic clock station, a rubidium atomic clock is installed, and GNSS antenna and receiver that are identical to those at the permanent stations used for the analysis are installed. The result of the positioning showed that it was improved by up to about 1.3 cm in the N direction, about 0.8 cm in the E direction, and about 1.7 cm in the U direction when PRN24 was not used for the positioning. Therefore, in this study, PRN24 was not considered for the determination of thresholds.

When failure occurs in more than two satellites at the same time, the abnormality detection method suggested in Section 3.1 cannot detect them at once; and a case in which one value has a different sign without the occurrence of abnormality cannot be completely ruled out. Thus, it is necessary to eliminate the satellite with a failure by setting thresholds for each result. In this study, thresholds were finally selected based on the analysis results in Table 2 and the average and standard deviation of RMS for each permanent station, as summarized in Table 3. To evaluate the performance of the selected thresholds, error was artificially added, and it was then analyzed. In the case of the experiment method, the satellite elevation angle was divided into 10 degree intervals, and 0.1 cycles were added to L1 and L2, respectively. In the case of the artificial error addition, the values jumped to about 0.0015 m for the acceleration, about 0.01 m for the ramp, and about 0.006 m for the step regardless of the satellite elevation angle
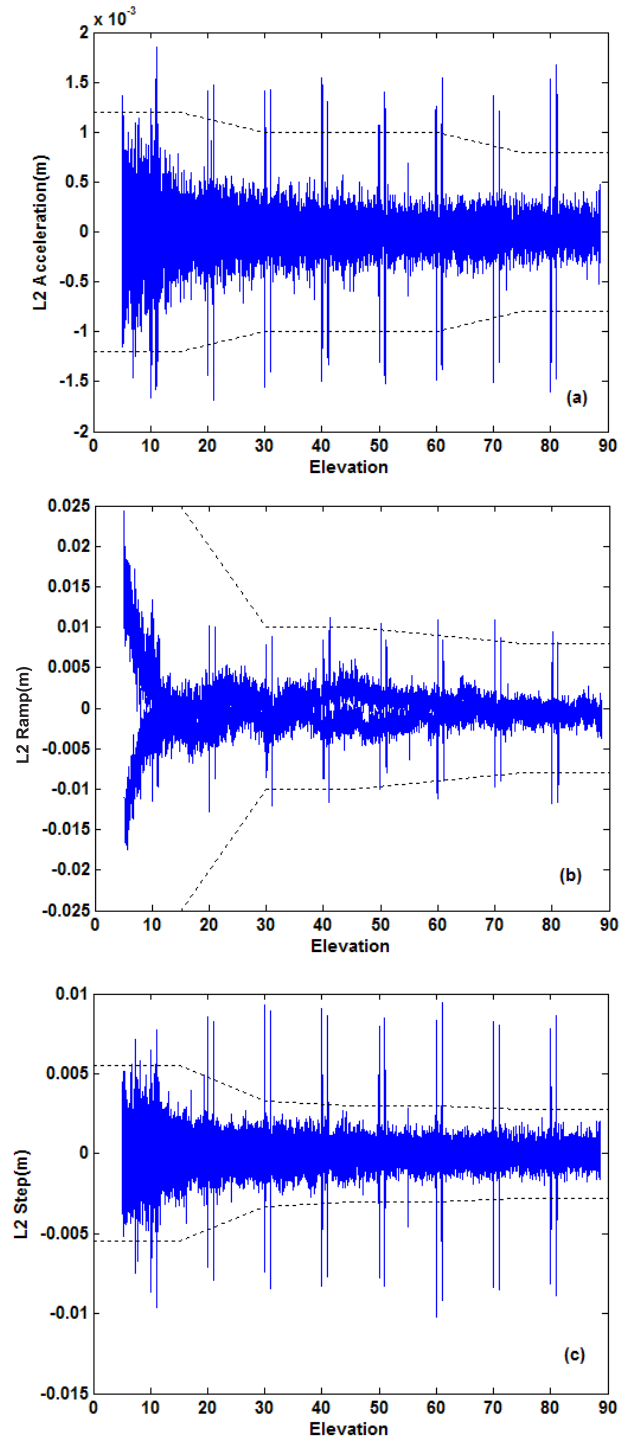
Fig. 6. Evaluation of the threshold of the L2's acceleration (a), ramp (b), and step (c) at GNJ.

as shown in Fig. 6. There was slight difference for each satellite, but the added error could be detected in most experiment results when the satellite elevation angle was more than 20 degrees. In addition, the value jumped to the + direction when the added error was larger than the existing measurement, and to the - direction when it was smaller.

4. CONCLUSIONS

In this study, the carrier acceleration-ramp-step test was carried out, and the results were compared and analyzed. When the carrier acceleration-ramp-step test is performed using broadcast ephemeris, the geometry range and satellite clock errors need to be adjusted based on the newly updated the broadcast ephemeris. For the result of the carrier acceleration-ramp-step test, RMS was analyzed by dividing the satellite elevation angle into 15 degree intervals. The result showed that the largest difference was observed at the satellite elevation angle of 5 to 15 degrees; and for the remaining satellite elevation angles, the test value decreased as the satellite elevation angle increased although the trend was gentle. In the carrier acceleration-ramp-step test, when failure occurred in a specific satellite, the jump of the value was the largest compared to those of the other satellites; and the values of the other satellites without a failure jumped in the opposite direction. When one cycle slip which is the minimum unit of a cycle slip was artificially added in order to evaluate the cycle slip detection performance of the carrier acceleration-ramp-step test, abnormalities could be detected in the acceleration, ramp, and step. In this study, seven-day carrier acceleration-ramp-step test was performed, and thresholds for the failure detection of carrier phase measurement were suggested. When 0.1 cycles were artificially added by dividing the satellite elevation angle into 10 degree intervals in order to evaluate the performance of the selected thresholds, the added error could be detected in the acceleration, ramp, and step. However, the thresholds suggested in this study are results obtained in general conditions. Therefore, for further generalization, additional studies need to be performed such as an analysis of the data directly affected by ionospheric and tropospheric errors (e.g., ionospheric storm or typhoon) and a long-term analysis.

ACKNOWLEDGMENTS

REFERENCES

Gang, X. 2004, Optimal On-Airport Monitoring of The Integrity of GPS-Based Landing Systems, PhD Dissertation, Stanford University

Hofmann-Wellenhof, B., Lichtenegger, H., & Wasle, E. 2008, GNSS: Global Navigation Satellite System: GPS, GLONASS & More (Wien: Springer-Verlag), http://dx.doi.org/10.1007/978-3-211-73017-1

Koenig, M. 2010, Optimizing The Decision Rule of A GPS Integrity Monitoring System for Improved Availability, PhD Dissertation, Stanford University

Lee, E.-S., Son, M., Son, E., Ahn, J.-S., Cho, D.-J., et al. 2013, Design and Validation of Integrity Risk Architecture for GNSS-Based Positioning using Multiple Receiving Stations, Journal of Cadastre, 43, 95-111, http://www.lx.or.kr/ebook/03study/siri2013_2/EBook.htm

Son, E. 2013, Accuracy Improvement of Long-range GPS L1 Relative Positioning using Regional Ionospheric and Tropspheric Grid Models, Master's Thesis, Inha University

Son, M., Son, E., Lee, E.-S., Heo, M.-B., & Nam, G.-W. 2013, Configuration of Network Based GNSS Correction System for Land Transportation Navigation, Journal of The Korea Society for Aviation and Aeronautics, 21, 17-26, http://dx.doi.org/10.12985/ksaa.2013.21.4.017

Eunseong Son received a M.S. degree from Inha University in 2013. He is a researcher in the KARI. He is interested in Real-time GNSS Carrier phase-based relative positioning, Integer Ambiguity fixing, Quality Monitoring, etc.

Koon-Tack Kim received his B.S and M.S. degrees in the Geoinformatic Engineering from Inha University in 2010 and 2013, respectively. He has joined the Satellite Navigation Team at KARI since 2013 and his current research is the development of GNSS-based transportation technology.

Sung-Hyuck Im is a senior researcher in the KARI. He received Ph.D. degree from Konkuk University in 2011. He is interested in (Real-time) software GNSS receiver, Generation and processing of navigation signals, Vector-based signal processing, Anti-Jamming/Spoofing, Indoor Positioning, Navigation sensor integration, etc.

Moon Beom Heo received a B.S. in the Mechanical Engineering from Kyung-Hee University, Korea, in 1992, and the M.S. and Ph. D. degrees in the Mechanical and Aerospace Engineering from the Illinois Institute of Technology, Chicago, respectively, in 1997 and 2004. He is currently a head of the Satellite Navigation Team at the KARI. His work is focused on Global Navigation Satellite System and their augmentation.